

NACA TN 3300

CASE FILE  
COPY

# NATIONAL ADVISORY COMMITTEE FOR AERONAUTICS

TECHNICAL NOTE 3300

INVESTIGATION OF LIFT, DRAG, AND PITCHING MOMENT  
OF A  $60^\circ$  DELTA-WING—BODY COMBINATION  
(AGARD CALIBRATION MODEL B) IN THE  
LANGLEY 9-INCH SUPERSONIC TUNNEL

By August F. Bromm, Jr.

Langley Aeronautical Laboratory  
Langley Field, Va.



Washington  
September 1954

F

NATIONAL ADVISORY COMMITTEE FOR AERONAUTICS

---

TECHNICAL NOTE 3300

---

INVESTIGATION OF LIFT, DRAG, AND PITCHING MOMENT

OF A  $60^\circ$  DELTA-WING—BODY COMBINATION

(AGARD CALIBRATION MODEL B) IN THE

LANGLEY 9-INCH SUPERSONIC TUNNEL

By August F. Bromm, Jr.

SUMMARY

The lift, drag, and pitching-moment characteristics of the AGARD Calibration Model B as determined in the Langley 9-inch supersonic tunnel are presented at Mach numbers of 1.62, 1.94, and 2.41 and at a Reynolds number, based on body length, of approximately  $3.0 \times 10^6$ . The zero-lift drag data compared favorably with available data and were in the proper sequence for the effects of Reynolds number.

INTRODUCTION

During the early period of development of subsonic wind tunnels, important discrepancies in data from different testing facilities were found. Many of these difficulties were resolved by improved techniques, equipment, and data corrections. In order to reduce further the uncertainty of comparison of data from different sources, a program of testing the same model in the primary test facilities of the world was instituted (ref. 1). As a result of these tests, the subsonic wind tunnel has become a reliable source of information; any discrepancies which remain are fairly well understood. Now, the same problem has arisen with the supersonic wind tunnels which have been built in recent years, and interest has been expressed in a test program for supersonic facilities similar to that for the subsonic facilities.

It was decided at the Rome meeting of the Advisory Group for Aeronautical Research and Development (AGARD) of the North Atlantic Treaty Organization in December 1952 to encourage such a program of tests in supersonic wind tunnels.

The first configuration selected for this purpose (AGARD Calibration Model A) was a slender body of revolution. This configuration was



designed by the National Advisory Committee for Aeronautics and tested in earlier correlation tests of its own facilities. It is probably better known as the NACA RM-10 research missile. Reference 2 is a presentation of the zero-lift drag data for this configuration measured in several NACA wind tunnels and in flight. A second AGARD configuration was also selected at the Rome meeting and was designated AGARD Calibration Model B. It is a new configuration consisting of a wing-body combination. The specifications for both AGARD models may be found in reference 3.

The purpose of the present paper is to present the results of tests of this new configuration (AGARD Calibration Model B) in the Langley 9-inch supersonic tunnel. The measurements included lift, drag, and pitching moment over an angle-of-attack range of  $\pm 6^\circ$ . The zero-lift base drag of this model was also measured. Tests were conducted at a Reynolds number, based on body length, of approximately  $3.0 \times 10^6$  at Mach numbers of 1.62, 1.94, and 2.41.

#### SYMBOLS

$C_D$	drag coefficient, $\frac{D}{qS}$
$C_{D_{\min}}$	minimum drag coefficient (zero lift and zero base drag)
$C_{D_b}$	base-drag coefficient, $P_b \frac{S_b}{S}$
$\Delta C_D$	rise in drag coefficient above minimum, $C_D - C_{D_{\min}}$
$C_L$	lift coefficient, $\frac{L}{qS}$
$C_{L_\alpha} = \left( \frac{\partial C_L}{\partial \alpha} \right)_{\alpha=0^\circ}$	
$C_m$	pitching-moment coefficient, $\frac{\text{Pitching moment}}{qS\bar{c}}$
$C_{m_\alpha} = \left( \frac{\partial C_m}{\partial \alpha} \right)_{\alpha=0^\circ}$	
$c$	wing root chord, measured along body center line
$\bar{c}$	mean aerodynamic chord, two-thirds root chord
$D$	drag

d	diameter of body
L	lift
$(L/D)_{\max}$	maximum lift-drag ratio
M	Mach number
$P_b$	base-pressure coefficient
q	dynamic pressure
R	Reynolds number, based on body length
r	radius of body at any station x
S	total wing area
$S_b$	total base area
t	maximum wing thickness
x	distance from nose along body axis
$x_{cp}$	distance from nose to center of pressure, body diameters
$\alpha$	angle of attack, deg

## APPARATUS

### Wind Tunnel

The Langley 9-inch supersonic tunnel is a continuous-operation closed-circuit tunnel in which the pressure, temperature, and humidity of the enclosed air can be regulated. Different test Mach numbers are provided by interchangeable nozzle blocks which form test sections approximately 9 inches square. Eleven fine-mesh turbulence-damping screens are installed in the relatively large area settling chamber ahead of the supersonic nozzle. The turbulence level of the tunnel is considered low, based on past turbulence-level measurements.

### Models

A drawing illustrating the construction details of the AGARD Calibration Model B and giving the pertinent dimensions is shown in



figure 1. A photograph of the unassembled model is shown in figure 2(a). The model is a wing-body combination with a fineness ratio of 8.5. The lifting surface is a  $60^\circ$  delta wing with a span four times the body diameter and has a symmetrical circular-arc section with a thickness ratio of 0.04 based on the streamwise chord. The body is a body of revolution having a cylindrical afterbody and a nose profile determined by the following equation which is obtained from the more general equation in reference 4:

$$r = \frac{x}{3} \left[ 1 - \frac{1}{9} \left( \frac{x}{d} \right)^2 + \frac{1}{54} \left( \frac{x}{d} \right)^3 \right] \quad (1)$$

The model was sting supported and had a sting-windshield arrangement as shown in figures 1 and 2(b). The straight portion of the sting windshield is about 2 body diameters in length; this is one-half a body diameter longer than is specified in reference 3. This modification seems justified because previous shroud-interference tests (turbulent boundary layer) have indicated that the critical length is about 2 body diameters in the Mach number range of these tests. The ratio of sting-windshield diameter to base diameter for the force tests conforms to the AGARD specifications, although this ratio is known to border on the critical. For the base-pressure tests, the ratio of sting diameter to model diameter was 0.375; and the ratio of the length of sting of constant diameter behind the model base to model diameter was 3.6. Accordingly, the sting effects of these tests are considered to be negligible. (See, for example, refs. 5 and 6.)

Four probes mounted as shown in figures 2(b) and 2(c) were used in the force tests to sense the pressure acting on the annulus of the model. This pressure and the pressure within the balance-enclosing box were employed to reduce the drag and the pitching moment to the condition of base pressure equal to stream pressure. A hollow, cylindrical sting vented to the area just inside the base of the model was employed in the base-pressure tests to sense the base pressures.

## TESTS

All tests were conducted at a Reynolds number of approximately  $3.0 \times 10^6$ , based on body length, or  $0.60 \times 10^6$ , based on the mean aerodynamic chord, and at Mach numbers of 1.62, 1.94, and 2.41. The force tests were made over an angle-of-attack range of  $\pm 6^\circ$ , and the base-pressure tests were conducted at an angle of attack of  $0^\circ$ . Fixed-transition tests were made with strips 3/16 inch wide by approximately 2/100 inch thick affixed as shown in figure 1. Measurements of lift,

drag, and pitching moment were made by means of an external six-component self-balancing mechanical balance. An optical system employing a small mirror mounted in the rear of the model was used to measure the angles of attack.

#### PRECISION OF DATA

The precision of the results has been evaluated by estimating the uncertainties in the balance measurements involved in a given quantity and combining these errors by a method based on the theory of least squares. A summary of these estimates follows:

Lift coefficient, $C_L$ . . . . .	$\pm 0.0004$
Drag coefficient, $C_D$ . . . . .	$\pm 0.001$
Base drag coefficient, $C_{D_b}$ . . . . .	$\pm 0.002$
Pitching-moment coefficient, $C_m$ . . . . .	$\pm 0.002$
Angle of attack, $\alpha$ . . . . .	$\pm 0.01$
Mach number, $M$ . . . . .	$\pm 0.01$

#### RESULTS AND DISCUSSION

The basic data are presented in the form of lift, drag, and pitching-moment coefficients, and the coefficients are based on the total wing area. Pitching-moment coefficients are based on the mean aerodynamic chord of the total wing and are referred to a point on the body axis two-thirds of the root chord from the apex of the wing. These data are presented for the condition of zero base drag in figure 3.

The parameters  $C_{L_\alpha}$ ,  $C_{m_\alpha}$ ,  $C_{D_{min}}$ , and  $C_{D_b}$  are presented in figure 4 as a function of Mach number. The slope of the lift curve decreases with Mach number as would be expected, and the slope of the pitching-moment curve increases with Mach number. The minimum-drag (zero-base-drag condition) values and the base-drag values for the model decrease slightly with Mach number. Figure 5 shows the movement of the center of pressure to be forward with Mach number.

The application of transition strips to the model has very little effect on  $C_{L_\alpha}$  but has the effect of slightly increasing  $C_{m_\alpha}$  at  $M = 1.62$  and slightly decreasing  $C_{m_\alpha}$  at  $M = 2.41$ . The largest effect of the transition strips is seen to be on the minimum drag. Figure 4 shows that the fixed-transition drag values are 75 to 90 percent greater



than the clean-model values. The increase in minimum drag may, for the most part, be attributed to an increase in skin-friction drag; a small portion may be due to an increase of pressure drag caused by the transition strips.

Figure 6 presents the variation of the lift-drag ratios with angle of attack. The curves of figure 6 were extrapolated to maximum values, and the extrapolated curves are shown in figure 7; this extrapolation appears justified because the experimental data seem to be very near a maximum. The maximum lift-drag ratio decreases slightly as the Mach number increases. A decrease of about 20 percent in the lift-drag ratios is experienced when transition strips are applied. This decrease is due primarily to the increase in drag which accompanies the use of fixed transition.

Figure 8 presents the variation of drag rise due to lift with Mach number. The values of drag rise for both the clean-model condition and the fixed-transition case at each Mach number were obtained by plotting  $\frac{\Delta C_D}{C_L^2}$  against angle of attack. These curves had an approximately zero slope except at very low angles of attack; therefore a single value for each curve is presented. The only data available for comparison with the present results are the zero-lift drag data of reference 7 which include base drag. (In ref. 7 AGARD Calibration Models A and B are referred to as AGARD Models 1 and 2, respectively.) For comparison purposes, the data of reference 7 have been extrapolated and are presented in figure 9. The drag coefficients for both the fixed-transition and the clean-model conditions are presented with and without base drag (fig. 9). The base-drag values are obtained from the separate base-drag tests mentioned previously. The present results and the extrapolation of the results of reference 7 compare favorably and are in the proper sequence for the effects of Reynolds number upon the skin-friction drag.

#### CONCLUDING REMARKS

The lift, drag, and pitching-moment characteristics of the AGARD Calibration Model B are presented at Mach numbers of 1.62, 1.94, and 2.41 and at a Reynolds number, based on body length, of approximately  $3.0 \times 10^6$ . The zero-lift drag data of the present tests compared favorably with available data and were in the proper sequence for the effects of Reynolds number.

Langley Aeronautical Laboratory,  
National Advisory Committee for Aeronautics,  
Langley Field, Va., July 27, 1954.

## REFERENCES

1. Anon.: Report on Aerofoil Tests at National Physical Laboratory and Royal Aircraft Establishment. R. & M. No. 954, British A.R.C., May 1925.
2. Evans, Albert J.: The Zero-Lift Drag of a Slender Body of Revolution (NACA RM-10 Research Model) As Determined From Tests in Several Wind Tunnels and in Flight at Supersonic Speeds. NACA TN 2944, 1953.
3. Anon.: Specifications for AGARD Wind Tunnel Calibration Models. AGARD Memo. AG4/M3 (Paris).
4. Roy, Maurice: Tuyères, Trompes, Fusées et Projectiles - Problèmes Divers de Dynamique des Fluides aux Grandes Vitesses. Pub. No. 203, Pub. Sci. et Tech. du Ministère de l'Air (Paris), 1947.
5. Perkins, Edward W.: Experimental Investigation of the Effects of Support Interference on the Drag of Bodies of Revolution at a Mach Number of 1.5. NACA TN 2292, 1951.
6. Chapman, Dean R.: An Analysis of Base Pressure at Supersonic Velocities and Comparison With Experiment. NACA Rep. 1051, 1951. (Supersedes NACA TN 2137.)
7. Piland, Robert O.: The Zero-Lift Drag of a  $60^\circ$  Delta-Wing—Body Combination (AGARD Model 2) Obtained From Free-Flight Tests Between Mach Numbers of 0.8 and 1.7. NACA TN 3081, 1954.



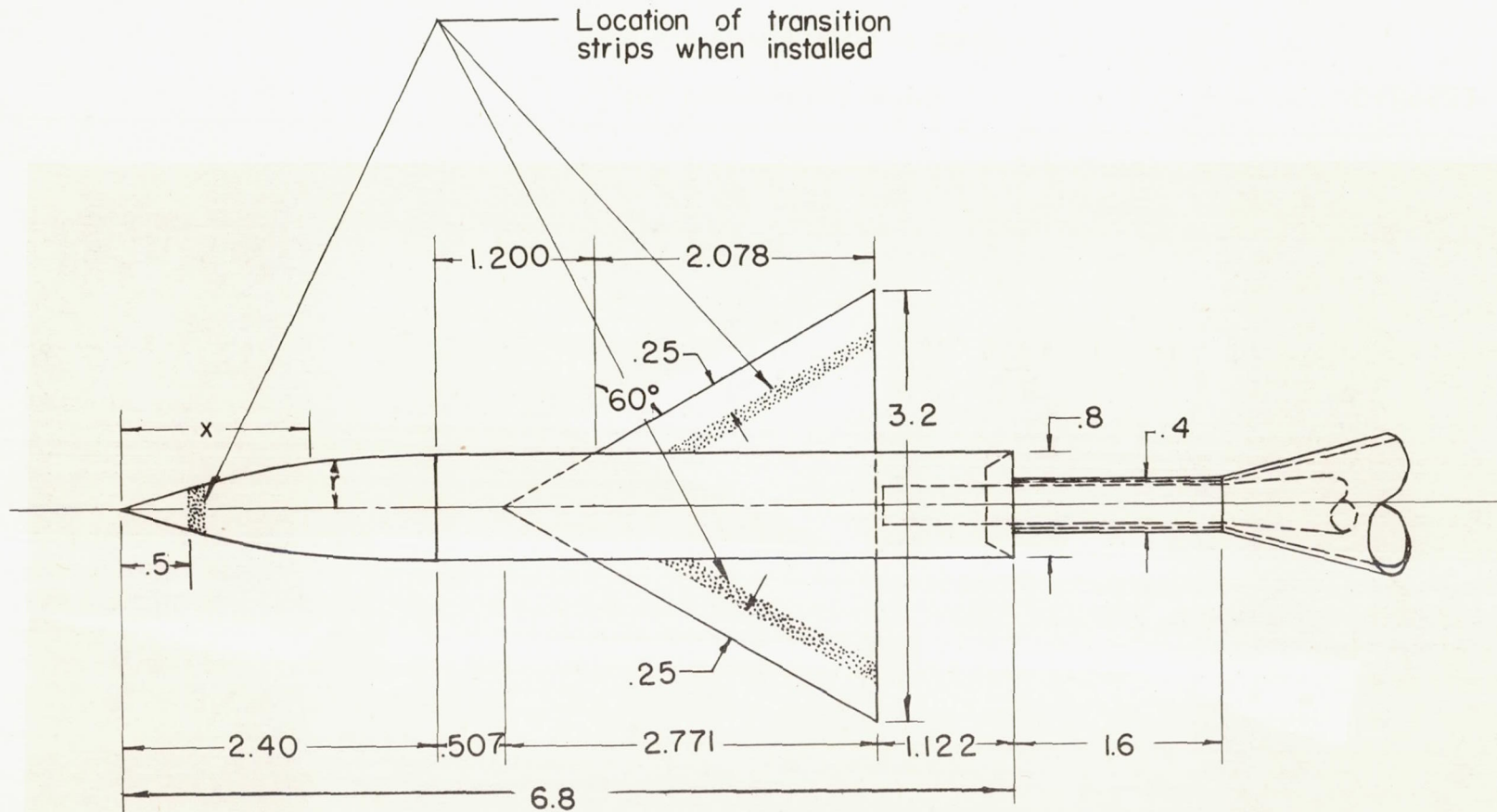
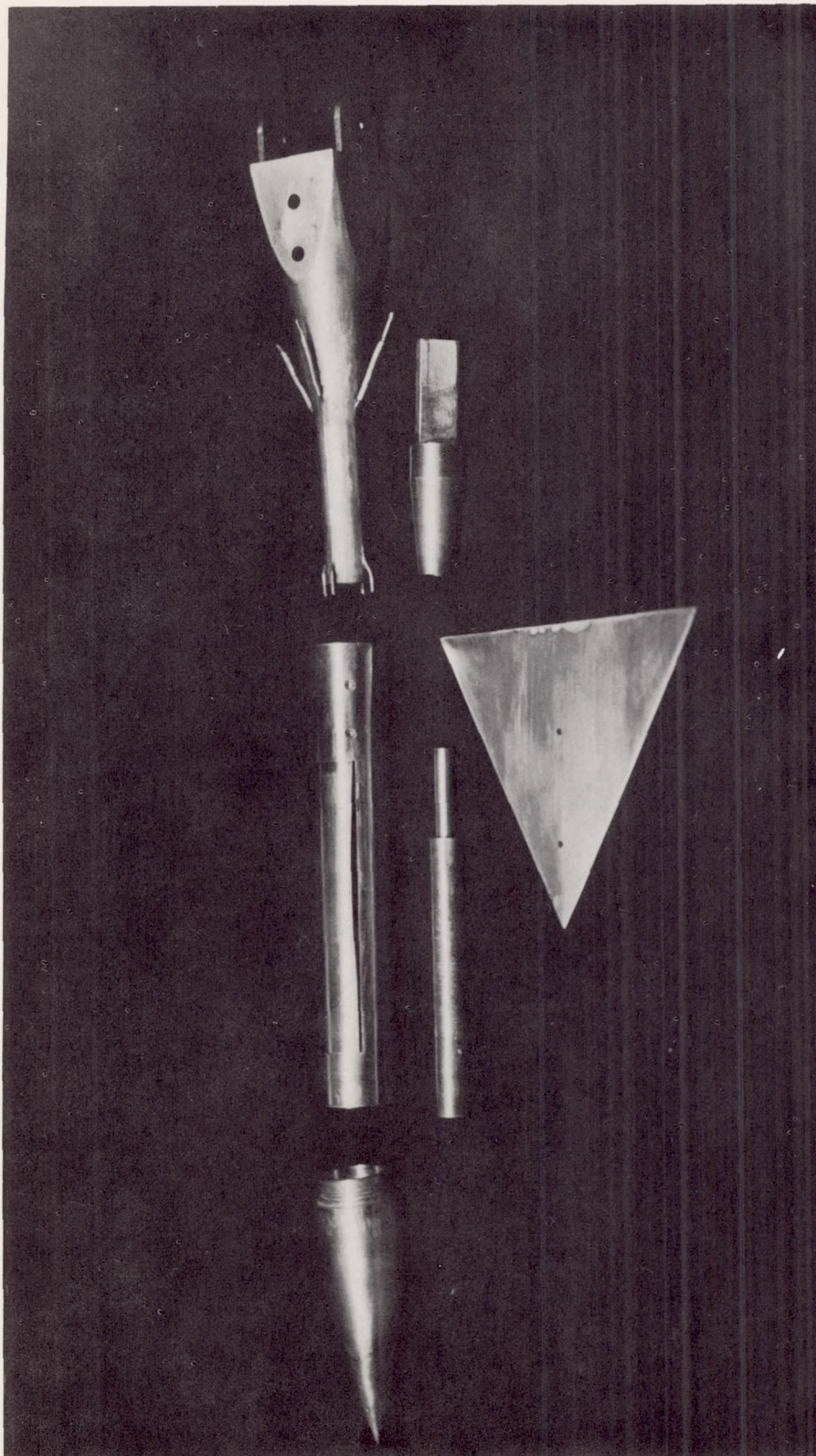


Figure 1.- Drawing of AGARD Calibration Model B. Equation of nose contour:

$$r = \frac{x}{3} \left[ 1 - \frac{1}{9} \left( \frac{x}{d} \right)^2 + \frac{1}{54} \left( \frac{x}{d} \right)^3 \right]. \quad \text{All dimensions are in inches unless otherwise noted.}$$

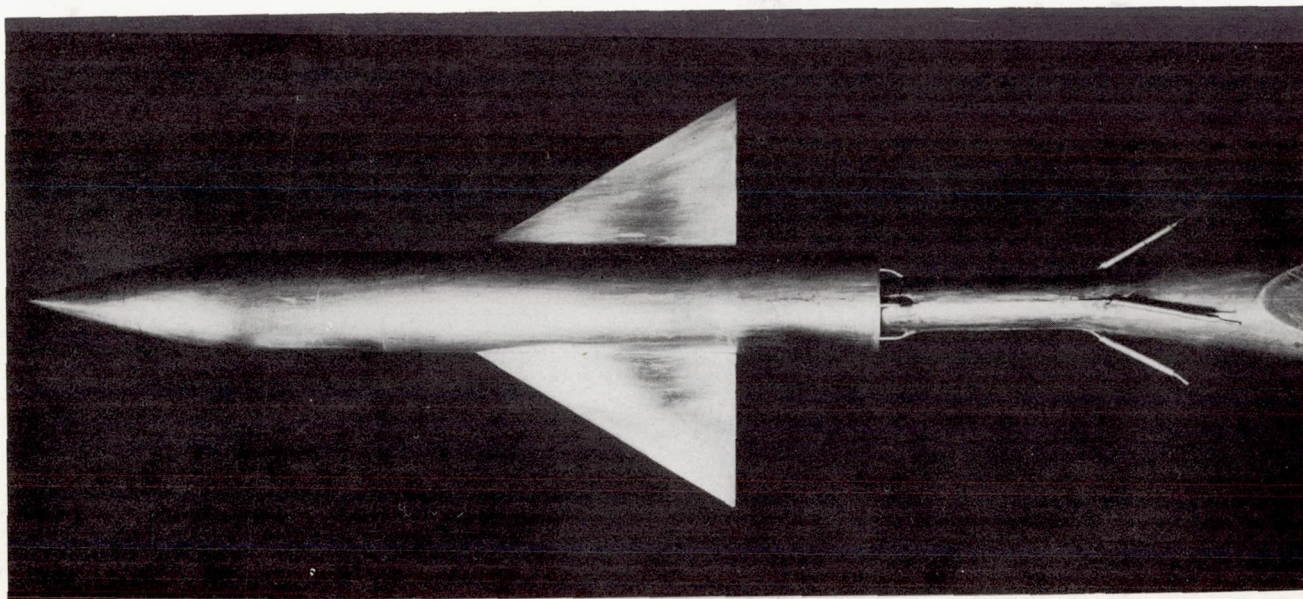


(a) Unassembled model.

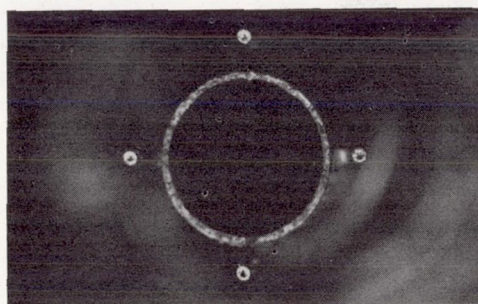
Figure 2.- Photographs of model.

L-85621





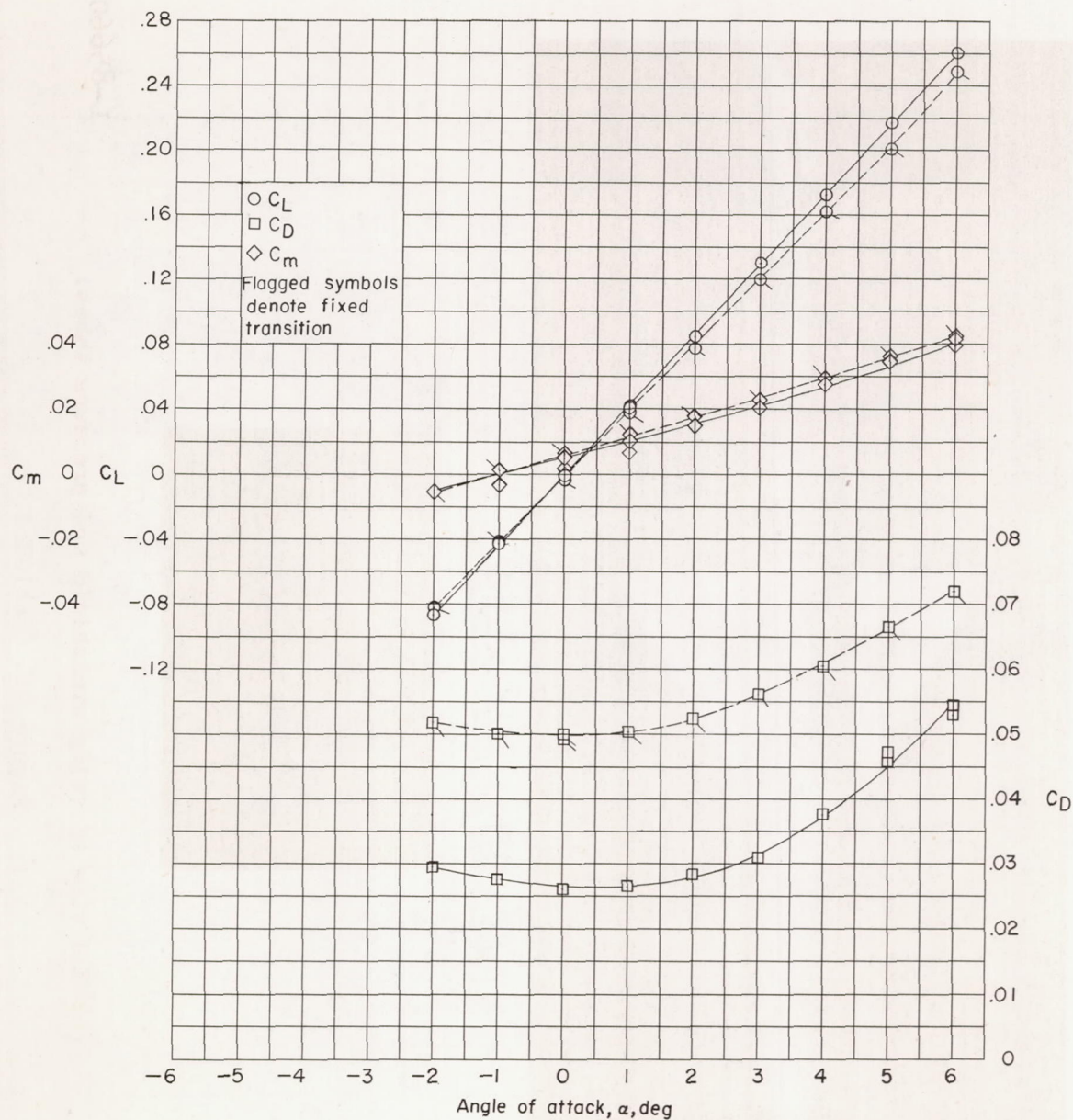
(b) Model and sting windshield assembled on sting.



(c) End view of sting windshield and pressure tubes.

Figure 2.- Concluded.

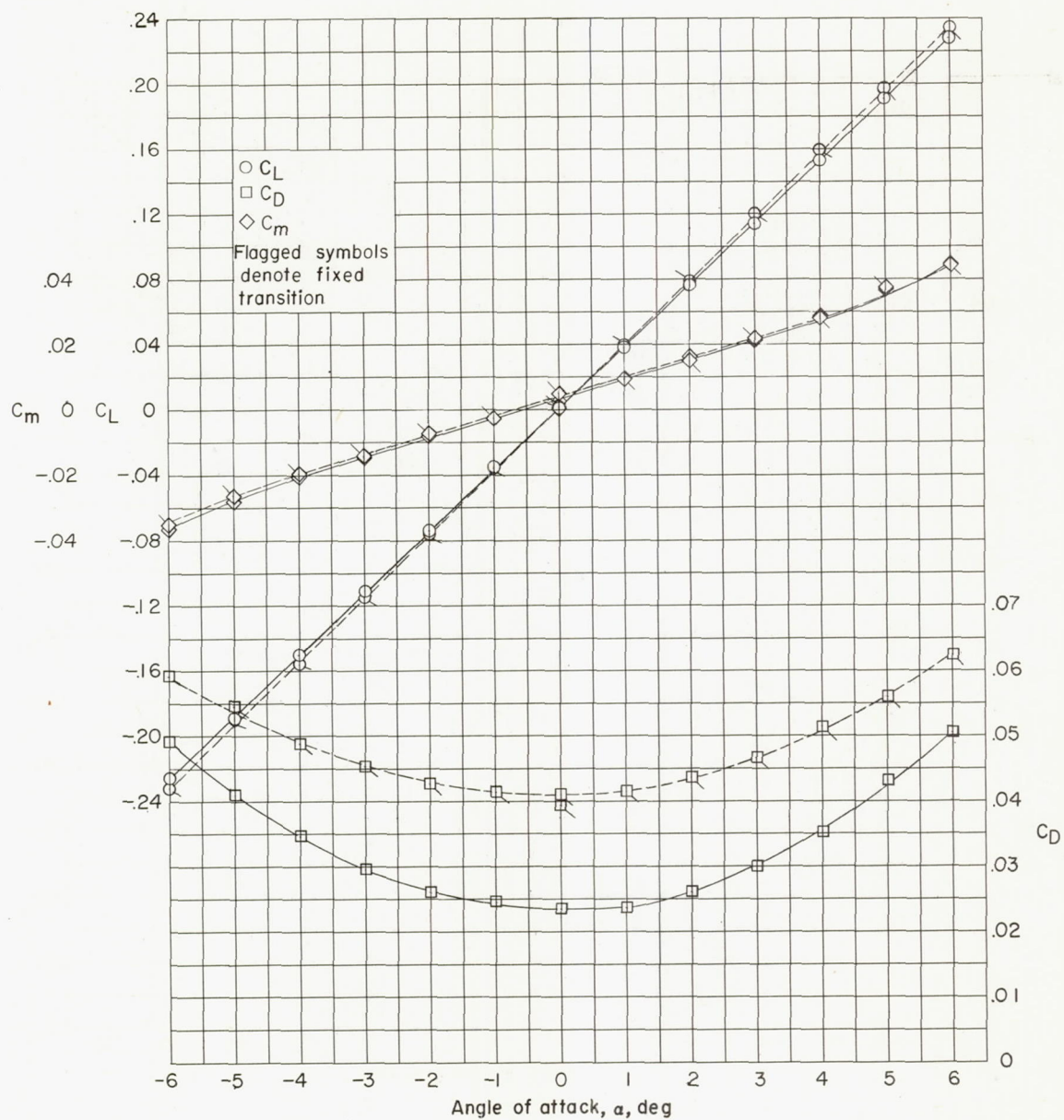
L-85660



(a)  $M = 1.62$ .

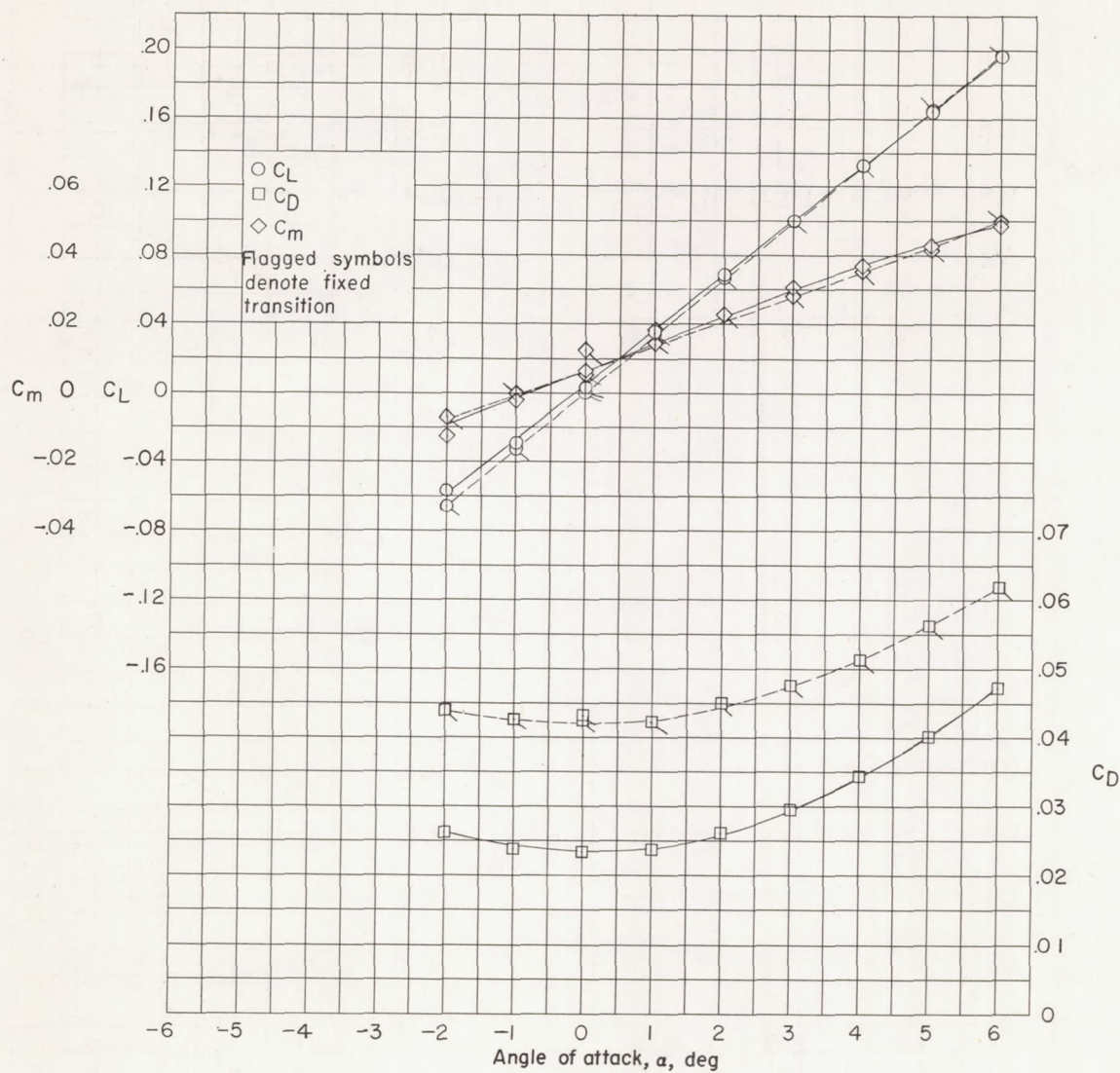
Figure 3.- Variation of lift, drag, and pitching moment with angle of attack.  $C_{D_0} = 0$ .





(b)  $M = 1.94$ .

Figure 3.- Continued.



(c)  $M = 2.41$ .

Figure 3.- Concluded.



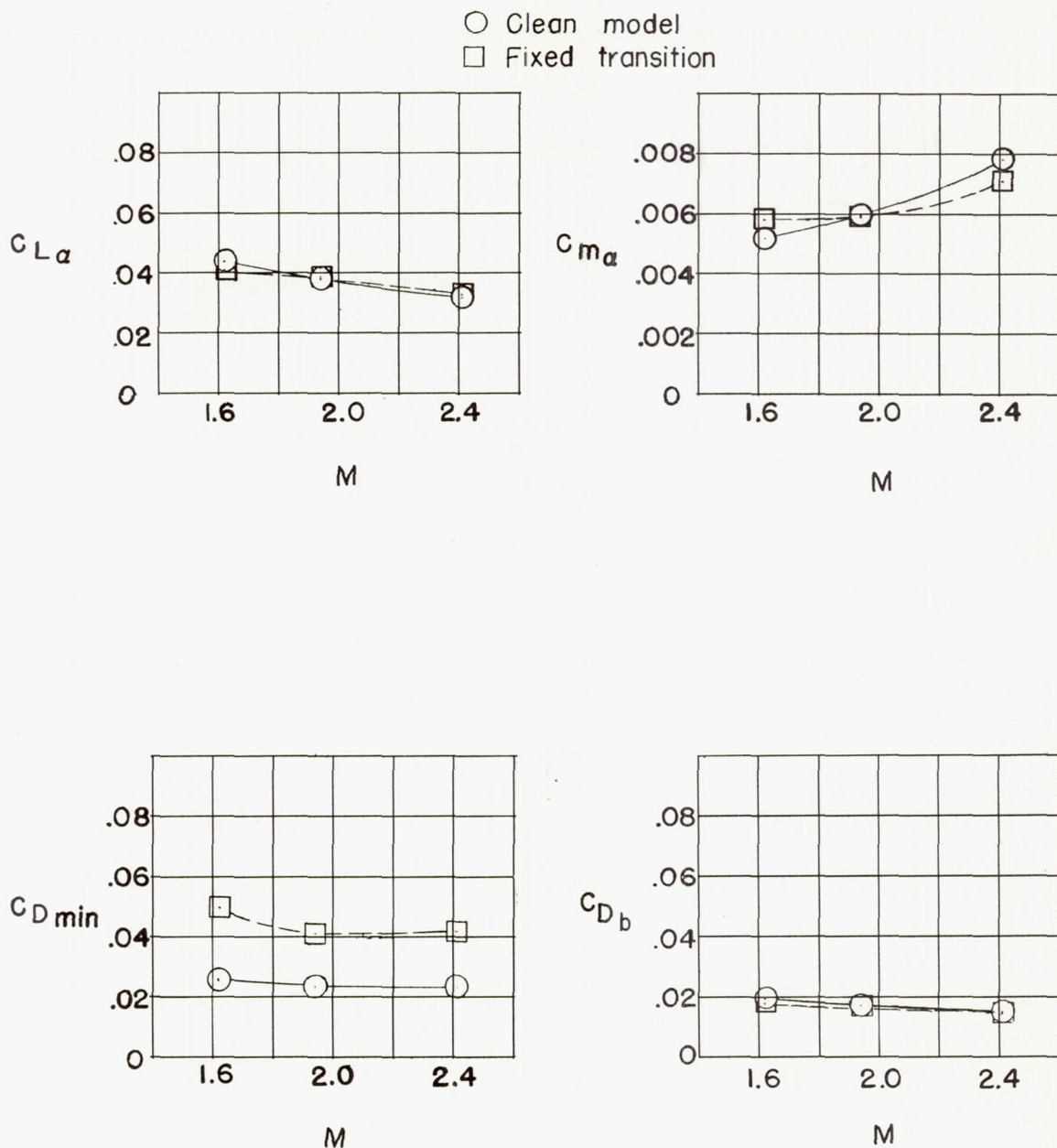


Figure 4.- Variation of the aerodynamic characteristics with Mach number.

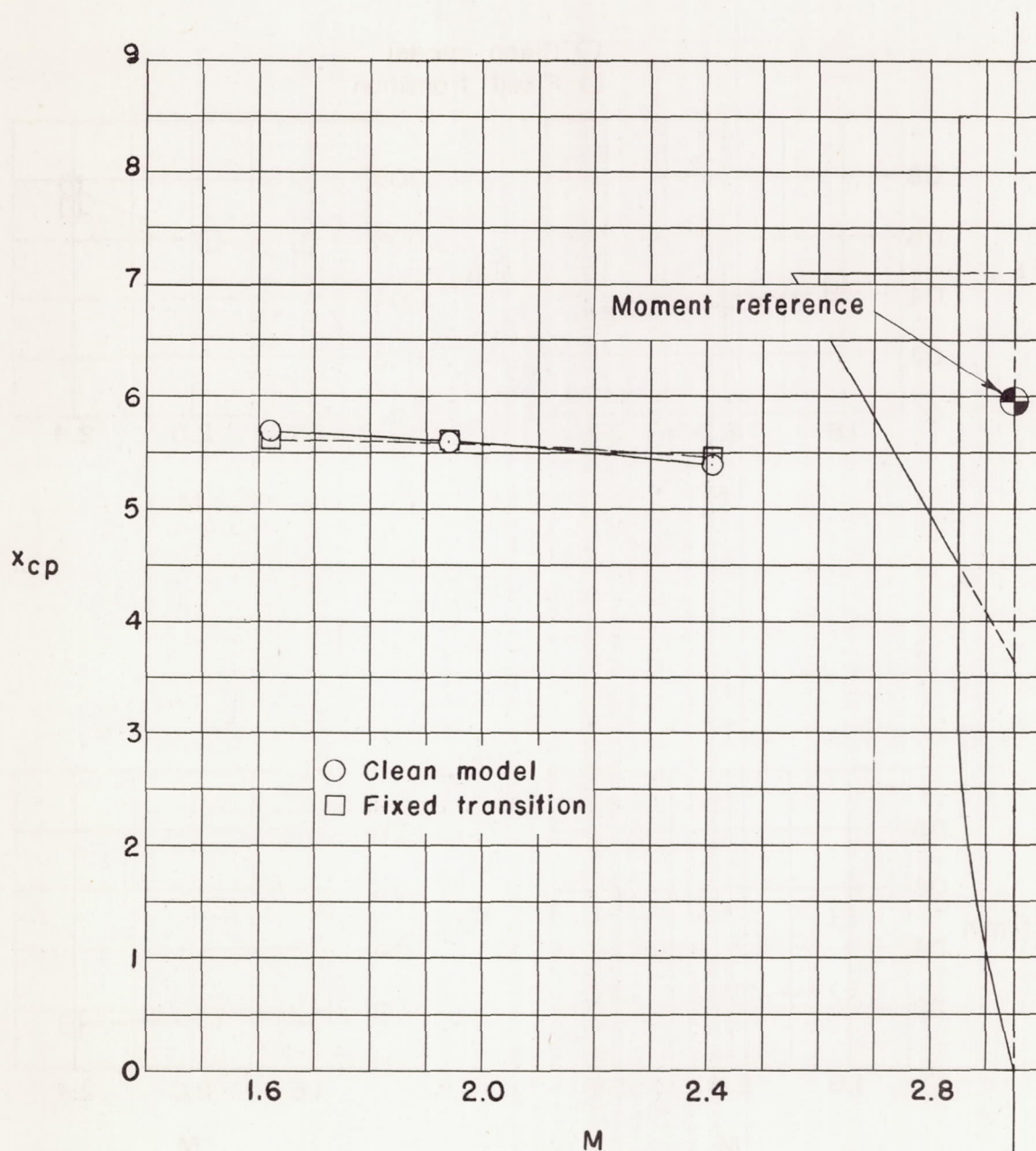


Figure 5.- Variation of center of pressure with Mach number.



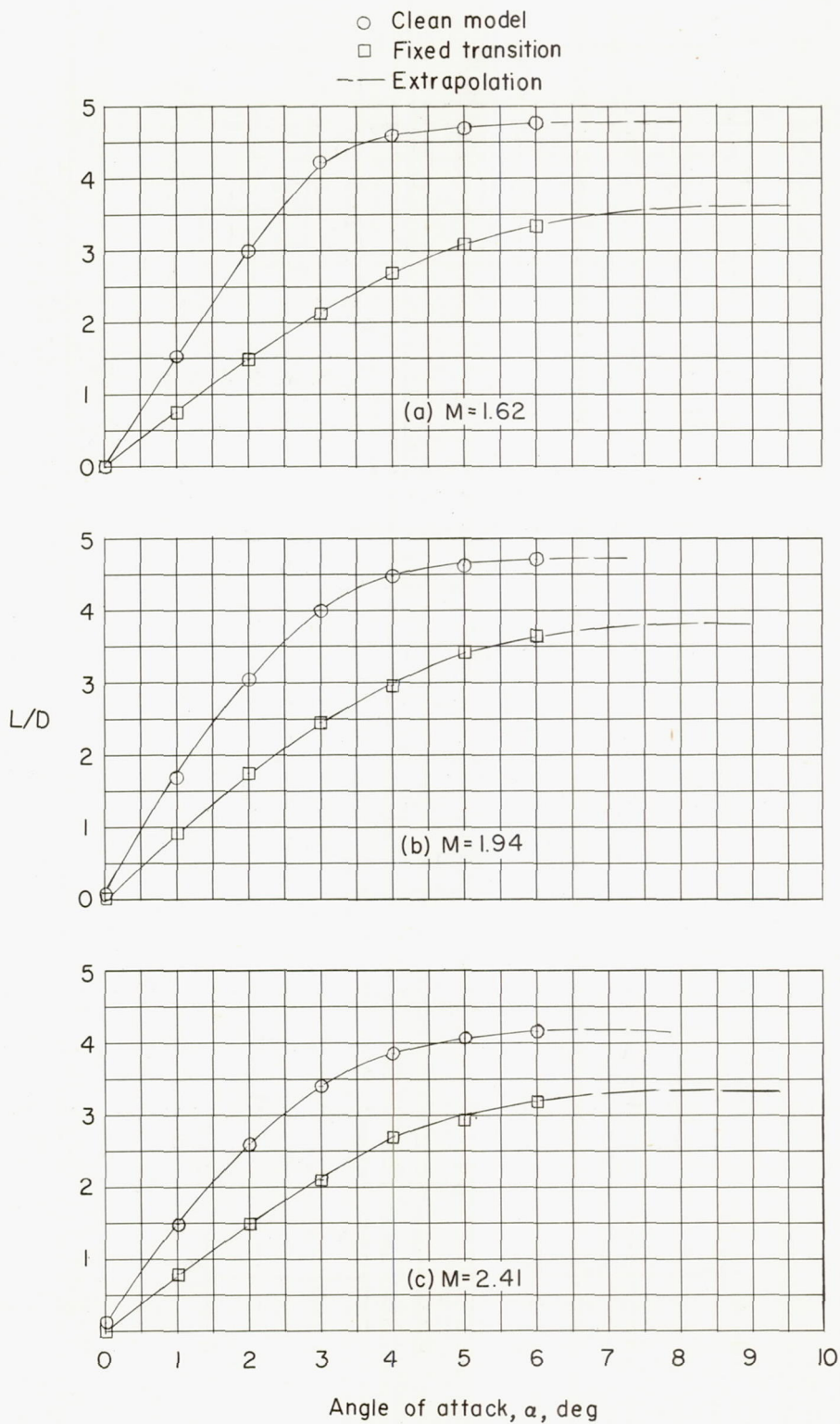


Figure 6.- Variation of  $L/D$  with angle of attack.

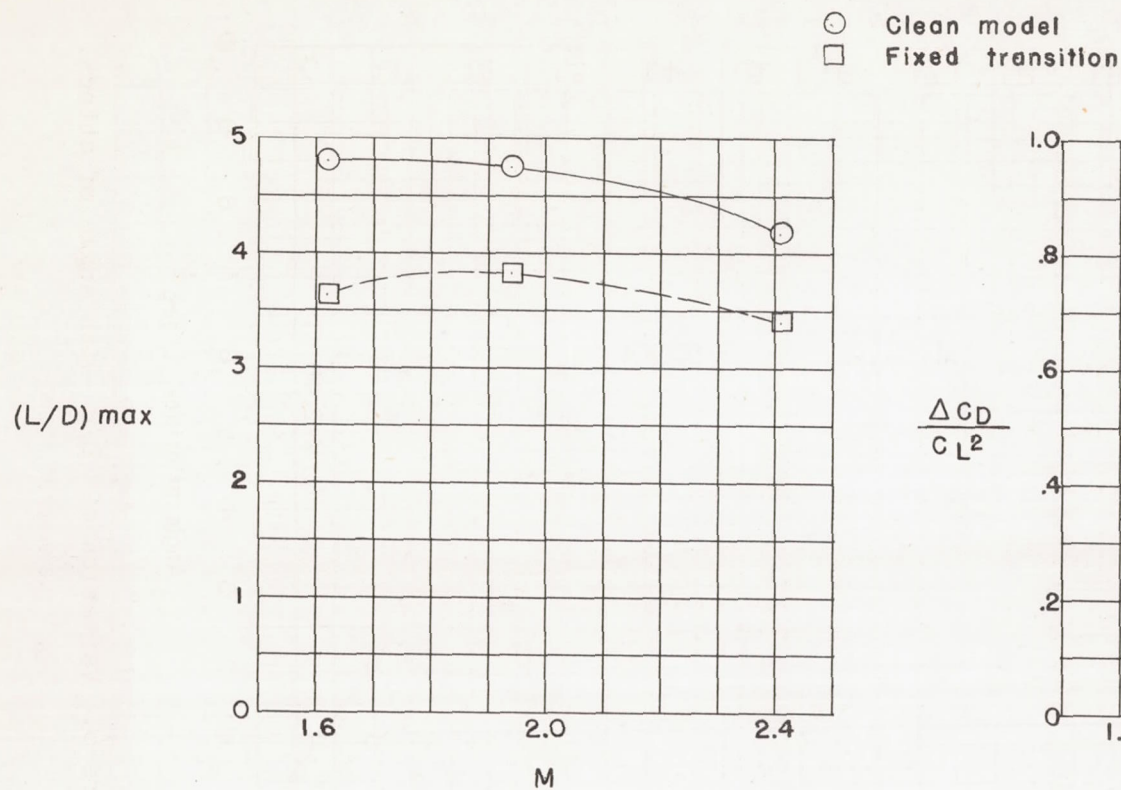


Figure 7.- Variation of  $(L/D)_{\max}$  with Mach number.

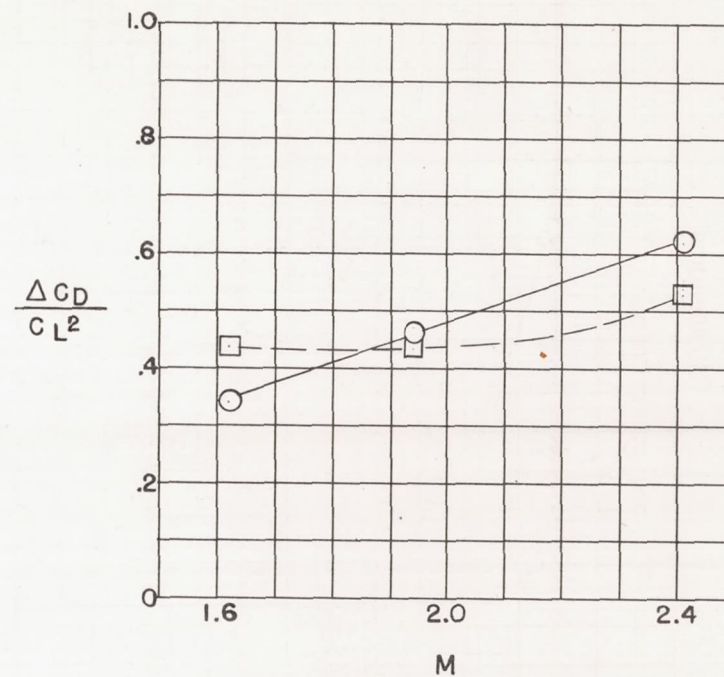


Figure 8.- Variation of the drag rise due to lift with Mach number.



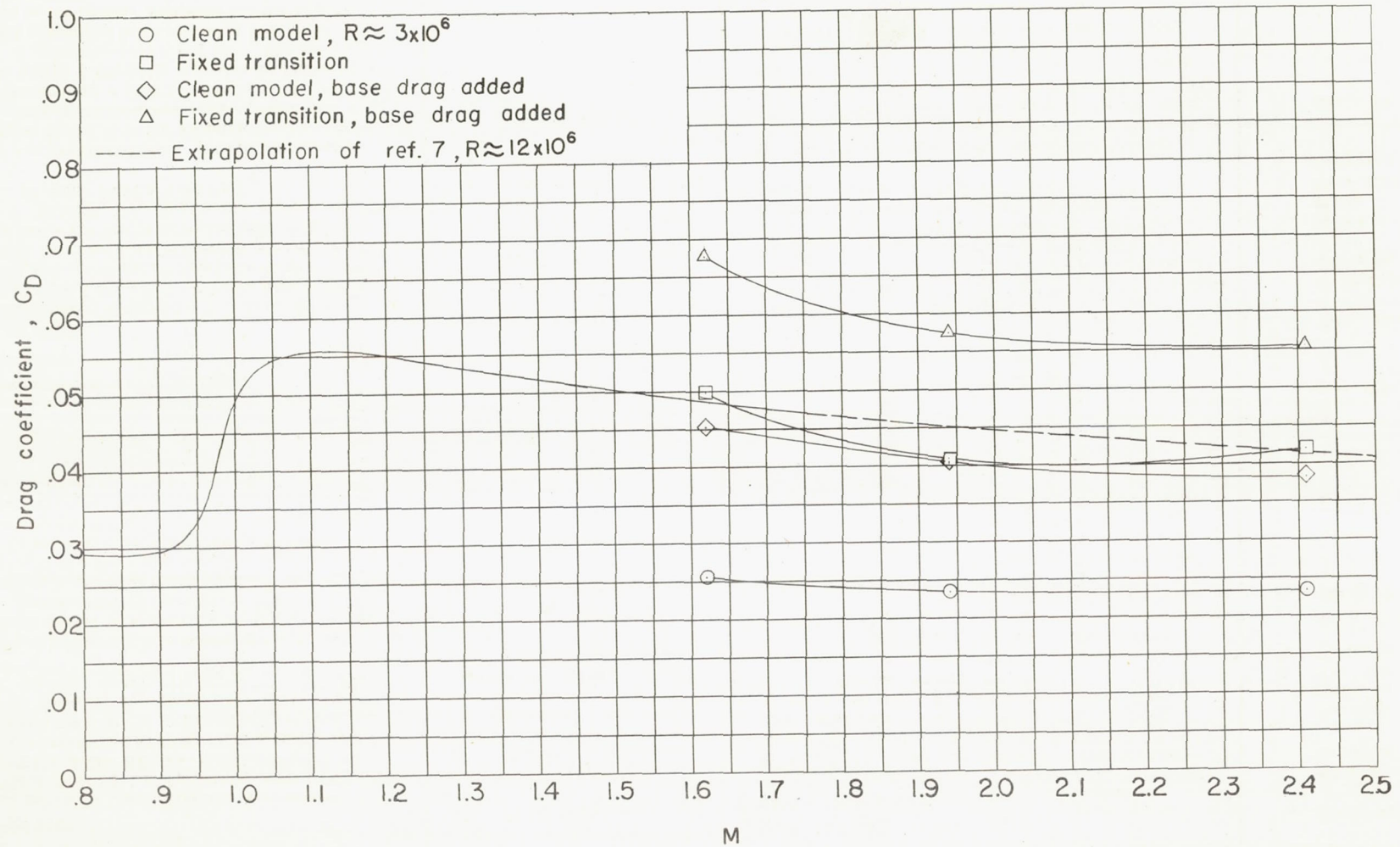


Figure 9.- Variation of drag coefficient at zero lift with Mach number.